DOI: 10.1002/ejic.200700694

New Mixed-Metal Aggregates Derived From Dinickel Complexes on a 2-Formylphenolate Template: Counteranion Dependent Formation of 1D Chain and Discrete $NaNi_2$ Complexes

Alok Ranjan Paital,[a] Masahiro Mikuriya,[b] and Debashis Ray*[a]

Keywords: Mixed-metal complexes / Imidazolidine / Dinuclear Ni^{II} complexes / Crystal structure / Magnetic properties

The combination of 2-formylphenol (Hfp) and the dinucleating ligand H_3L {2-(2′-hydroxyphenyl)-1,3-bis[4-(2-hydroxyphenyl)-3-azabut-3-enyl]-1,3-imidazolidine} with $Ni(NO_3)_2 \cdot 6H_2O$ leads to the self-assembly of a Ni_2 complex capable of showing anion dependent Na^+ coordination. The terminal aqua coordinated $[Ni_2(fp)L(H_2O)] \cdot 3H_2O$ (**1**·$3H_2O$) neutral fragment, formed in the absence of any Na^+ source, produces a 1D chain complex $[\{Ni_2(fp)L(N_3)(Na)(H_2O)\} \cdot 5H_2O]_n$ (**2**·$5H_2O)_n$ and a discrete $NaNi_2$ complex $[Ni_2(fp)L(Na)(H_2O)_2] \cdot ClO_4 \cdot H_2O$ (**3**·ClO_4·H_2O) through its weak oxophilic interaction with a Na^+ cation of the coordinated trisphenolate unit of L^{3-} as observed in metallacrowns. In complexes **2** and **3**, the Ni^{II} ions are coupled ferromagnetically to yield $S = 2$ ground states. The magnetic data can be modeled by using the Van Vleck equation incorporating intermolecular interactions.

Introduction

Mixed-metal aggregates, involving intimate association of Na^+ ions with transition-metal clusters,[1] have recently drawn attention because of their interesting structural and magnetic properties and also because of their contribution towards the understanding of molecular recognition in biological systems.[2] Structural characterization of Na^+- and Ca^{2+}-bound Mn_4 clusters has shown promise in recent times for their relevance in understanding the oxygen-evolving center of photosystem II (PS II).[3] Salicylaldimines[4] and its substituted analogues[5] are known to exhibit simultaneous coordination of transition and alkali metal ions. In recent years, we and others were interested in the multinucleating properties of the ligand H_3L {2-(2′-hydroxyphenyl)-1,3-bis[4-(2-hydroxyphenyl)-3-azabut-3-enyl]-1,3-imidazolidine, Scheme 1} for various reasons, which include their importance in bioinorganic chemistry, molecular magnetism, and catalysis.[6–11]

During the course of these investigations, we observed that under certain conditions, complexation reactions with Mn^{III}, Fe^{III}, Co^{III}, or Cu^{II} leads to the hydrolysis of the imidazolidine ring[12–14] and even the destruction of the imine bond.[15] The instability of some of the dinuclear Ni^{II} complexes of a related ligand was also reported.[16] While investigating the use of 2-formylphenol (Hfp) as a hydrolysis-inhibiting template ligand in nickel phenolate chemistry of H_3L, we recently observed that hydrolysis can be prevented by use of the appropriate *o*-formylphenols as coligands, namely 2-formylphenol (Hfp, Scheme 1, right) and 2,6-diformyl-4-methylphenol (Hdfp).[17] The terminal single-water–coordinated, neutral complex $[Ni_2L(fp)(H_2O)] \cdot 3H_2O$ (**1**·$3H_2O$) was synthesized on the formylphenolate template as reported recently.[17] The substitution reaction of the coordinated water molecule was tested in a reaction with NaN_3 and provides a 1D chain complex $\{[Ni_2L(fp)(N_3)(Na)(H_2O)] \cdot 5H_2O\}_n$ (**2**·$5H_2O)_n$ that links Ni_2 neutral fragments by $(H_2O)NaN_3$ units. The role of the anion, which has the potential to remove the terminal water molecule coordinated to one of the nickel ions, for the metallacrown-ether-like coordination of the Na^+ cation through the coordinated trisphenolate unit of L^{3-} is further verified by a second reaction of **1** with $NaClO_4 \cdot H_2O$ that forms $[Ni_2L(fp)(Na)(H_2O)_2] \cdot ClO_4 \cdot H_2O$ (**3**·ClO_4·H_2O). In complex **3**, as the coordinated water molecule cannot be substituted by bulky perchlorate anion because of steric effects, it remains uncoordinated. These reactions constitute rare examples in which simultaneous incorporation of both

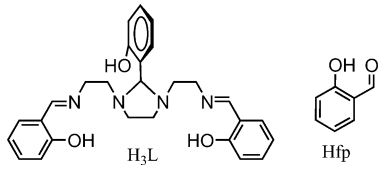

Scheme 1.

[a] Department of Chemistry, Indian Institute of Technology, Kharagpur 721302, India
Fax: +91-3222-82252
E-mail: dray@chem.iitkgp.ernet.in
[b] School of Science and Technology, Kwansei Gakuin University, 2-1 Gakuen 669-1337, Japan

Supporting information for this article is available on the WWW under http://www.eurjic.org or from the author.

cation and anion in a charge neutral complex is observed. The oxophilic nature of Na^+ allows its coordination to the trisphenolate unit first, after which anions are either incorporated or remain uncoordinated in order to provide 1D chain or discrete $NaNi_2$ complexes, respectively. The typical arrangement of L^{3-} around the Ni^{II} ions in **1** leads to the formation of a [–O–Ni–O–Ni–O–] moiety disposed so as to provide three *facial* oxygen donors that form distorted square-pyramidal and trigonal coordination environments around Na^+ cation, which is different from the most common octahedral coordination.[8,18]

Herein, we report the synthesis, crystallographic characterization, and magnetic properties of two different Na^+-bound Ni_2 complexes assembled on formylphenolate templates and with a coordinated capping dinucleating L^{3-} ligand. The anion-dependent binding of Na^+ ions leads to a novel 1D $Ni_2(O_3)$–Na–N_3–$Ni_2(O_3)$ chain and a discrete $NaNi_2$ complex.

Results and Discussion

Syntheses, Reactivity, and Spectroscopic Characterizations

The ligand H_3L {2-(2′-hydroxyphenyl)-1,3-bis[4-(2-hydroxyphenyl)-3-azabut-3-enyl]-1,3-imidazolidine} was prepared according to a literature procedure.[19] The aqua Ni_2 complex **1** was prepared on a 2-formylphenolate (fp^-) template by using $Ni(NO_3)_2{\cdot}6H_2O$ and H_3L in MeOH solvent under refluxing conditions following a standardized procedure reported by us.[17] In that report we noticed that in solution, H_3L is unstable during reactions with nickel(II) salts and crystals of the hydrogen-bonded dimer of the mononuclear complex cations $[Ni(HL')]_2^{2+}$ were produced in low yield (H_2L' is the hexadentate proligand formed from the imidazolidine ring hydrolysis of H_3L).[17] Since the 2-formylphenolate (fp^-) moiety is generated from the hydrolysis of L^{3-}, the ligand decomposition could be inhibited in the presence of the former as a template. The process of ligand hydrolysis, however, is inhibited completely if Hfp is mixed beforehand with a solution of $Ni(NO_3)_2{\cdot}4H_2O$, which presumably leads to the formation of intermediate **A** (Scheme 2). This results in the formation of complex **1** after addition of H_3L, where the deprotonated 2-formylphenolate (fp^-) behaves as a tridentate bridging ligand that stabilizes the Ni^{II}_2 complex. In the present work, we have studied the anion-dependent metalloligand behavior of **1** towards the binding of the sodium ion. A general procedure was followed for the synthesis of complexes **2** and **3** by using two sources of Na^+ such as NaN_3 and $NaClO_4{\cdot}H_2O$ in MeCN at room temperature in air. The reaction of complex **1** with NaN_3 in a 1:1 or 1:2 molar ratio in CH_3CN/MeOH (1:1) solvent mixture with stirring in air gives a green microcrystalline complex **2** in 78% yield (Scheme 2).

Addition of excess NaN_3 could not displace the formylphenolate template from **1** to produce any azido-bridged dinickel complex. The reaction of complex **1** with $NaClO_4{\cdot}H_2O$ in CH_3CN/EtOH (1:1) whilst stirring in air at room temperature yields **3** as a green microcrystalline com-

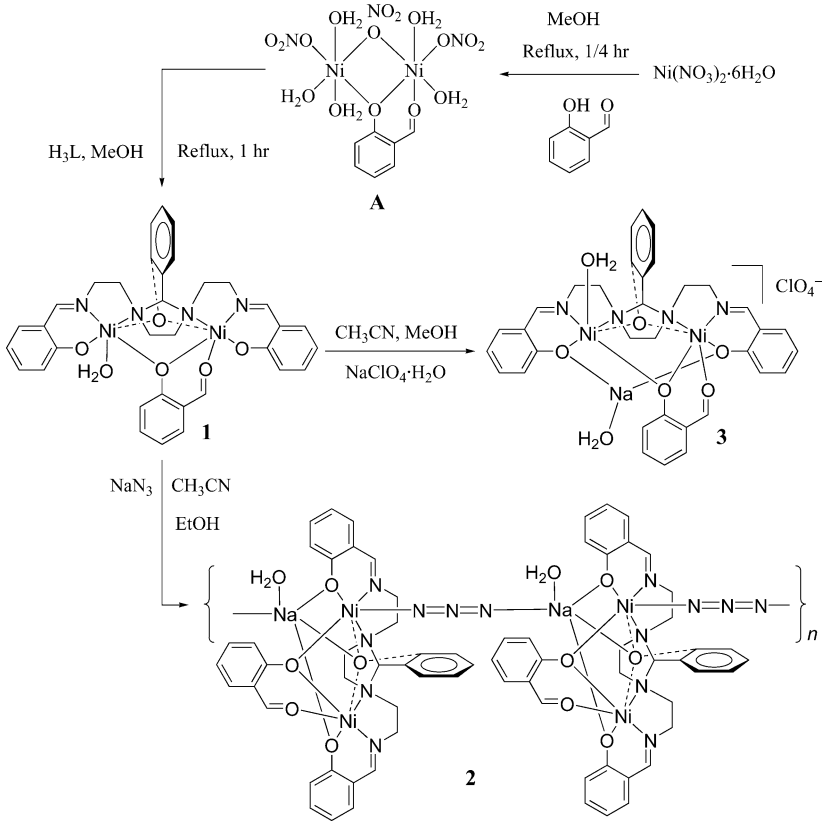

Scheme 2.

plex in 75% yield. Both of these reactions show that oxophilic Na^+ ions could be attached at the trisphenolate metaloligand site of the Ni_2L fragment and that charge neutrality is maintained by anions. All the compounds are insoluble in water and separate directly from the reaction mixture, and were thoroughly washed with water before characterization. The formulation of all the complexes is consistent with elemental and metal analysis and solution electrical conductivity data in CH_3CN. The molar conductivity values (Λ_M) are 16 and 130 $\Omega^{-1}cm^2\,mol^{-1}$ (28 °C) and are consistent with the charge neutral and 1:1 electrolyte behavior of **2** and **3**, respectively. FTIR and UV/Vis spectral analyses also confirm the formation of **2** and **3**.

Infrared Spectroscopy

The FTIR spectra of **2** and **3** show strong absorption bands at 1639 and 1642 cm^{-1}, respectively, which are characteristic of the coordinated C=N functionality of the ligand L^{3-}, and these values are slightly lowered in energy relative to that of the free ligand H_3L. Broad medium bands spanning the 3600 to 3200 cm^{-1} range with maxima at 3411 and 3421 cm^{-1} are observed, which can be assigned to ν(OH) stretching vibrations from both the metal-ion-coordinated and lattice water molecules in complexes **2** and **3**, respectively. Both the asymmetric and symmetric stretching vibrations are in this range. Strong bands at 1598 and 1600 cm^{-1} are observed, which correspond to ν(C=O) of the coordinated functionality of fp^- in complexes **2** and **3**, respectively. In addition, complex **2** shows a very strong sharp band at 2074 cm^{-1} for the $\nu_{as}(N_3^-)$ stretching band.[20] The FTIR spectrum of complex **3** contains the characteristic vibration at 1121 cm^{-1} for the uncoordinated tetrahedral perchlorate anion.[21]

Electronic Spectroscopy

Hexacoordination of the metal centers in **2** and **3** is also retained in solution as evidenced by the UV/Vis absorption spectra. The light green solution of complex **2** shows three broad electronic absorption bands at 932 (ν_1, ε = 90 $M^{-1}cm^{-1}$), 783 (ν_2, ε = 35 $M^{-1}cm^{-1}$) and 603 nm (ν_3, ε = 60 $M^{-1}cm^{-1}$). These can be assigned to the $^3A_{2g}(F)\rightarrow{}^3T_{2g}(F)$, $^3A_{2g}(F)\rightarrow{}^1E_{1g}(D)$, and $^3A_{2g}(F)\rightarrow{}^3T_{1g}(F)$ ligand-field transitions in accord with d^8 ions in near octahedral coordination environments.[22] Apart from these, two other bands at 375 (ε = 12605 $M^{-1}cm^{-1}$) and 271 nm (ε = 17235 $M^{-1}cm^{-1}$) are observed, which arise from charge-transfer transitions. Similarly, for complex **3**, bands at 922 (ε = 85 $M^{-1}cm^{-1}$), 783 (ε = 30 $M^{-1}cm^{-1}$), and 510 nm (ε = 55 $M^{-1}cm^{-1}$) are observed as a result of d–d transitions assigned to $^3A_{2g}(F)\rightarrow{}^3T_{2g}(F)$, $^3A_{2g}(F)\rightarrow{}^1E_{1g}(D)$, and $^3A_{2g}(F)\rightarrow{}^3T_{1g}(F)$ transitions, respectively. Apart from these, two other bands at 375 (ε = 12870 $M^{-1}cm^{-1}$) and 295 nm (ε = 14485 $M^{-1}cm^{-1}$) are observed for the charge-transfer transitions. The band arising from the $^3A_{2g}(F)\rightarrow{}^3T_{1g}(P)$ transition is probably hidden under the intense absorption bands in the near ultraviolet region of the spectrum at 375 nm.

Description of Structures

Green blocklike single crystals suitable for X-ray structure determination were obtained by slow evaporation of CH_3CN and CH_3CN/EtOH (1:1) solutions of **2** and **3**, respectively, after a week. Atom labeling scheme and molecular views (ORTEP) of the complexes are shown in Figures 1–9. Selected interatomic distances and angles are collected in Table 1 and Table 2.

Table 1. Selected interatomic distances [Å] and angles [°] for complex **2**.

Ni1–O1	1.989(8)	O1–Ni1–N2	174.0(4)
Ni1–N1	2.025(10)	N1–Ni1–N2	83.0(4)
Ni1–O4	2.041(7)	O4–Ni1–N2	95.1(3)
Ni1–O2	2.070(6)	O2–Ni1–N2	90.2(3)
Ni1–O5	2.099(8)	O5–Ni1–N2	91.7(3)
Ni1–N2	2.176(9)	N4–Ni2–O3	90.7(3)
Ni2–N4	1.997(8)	N4–Ni2–O4	173.8(3)
Ni2–O3	2.012(7)	O3–Ni2–O4	92.1(3)
Ni2–O4	2.082(6)	N4–Ni2–N5	91.5(4)
Ni2–N5	2.083(12)	O3–Ni2–N5	91.9(4)
Ni2–O2	2.103(7)	O4–Ni2–N5	93.8(4)
Ni2–N3	2.196(9)	N4–Ni2–O2	97.6(3)
Na1–O3	2.264(9)	O3–Ni2–O2	88.2(3)
Na1–O1	2.301(9)	O4–Ni2–O2	77.1(3)
Na1–N7	2.364(19)	N5–Ni2–O2	170.9(4)
Na1–O2	2.377(8)	N4–Ni2–N3	83.3(3)
Na1–O6	2.513(16)	O3–Ni2–N3	171.8(3)
		O4–Ni2–N3	93.3(3)
Ni1–O4–Ni2	99.2(3)	N5–Ni2–N3	93.8(4)
Ni1–O2–Ni2	97.6(3)	O2–Ni2–N3	87.0(3)
O1–Ni1–N1	91.0(4)	O3–Na1–O1	127.9(4)
O1–Ni1–O4	90.9(3)	O3–Na1–N7	114.1(5)
N1–Ni1–O4	175.6(4)	O1–Na1–N7	118.0(5)
O1–Ni1–O2	90.5(3)	O3–Na1–O2	76.2(3)
N1–Ni1–O2	105.2(3)	O1–Na1–O2	76.1(3)
O4–Ni1–O2	78.7(3)	N7–Na1–O2	122.3(5)
O1–Ni1–O5	88.9(3)	O3–Na1–O6	91.9(5)
N1–Ni1–O5	88.3(4)	O1–Na1–O6	83.0(5)
O4–Ni1–O5	87.8(3)	N7–Na1–O6	96.7(7)
O2–Ni1–O5	166.5(3)	O2–Na1–O6	140.9(6)

$\{[Ni_2(fp)L(N_3)(Na)(H_2O)]\cdot5H_2O\}_n$ $(2\cdot5H_2O)_n$

The molecular structure of **2** in Figure 1 reveals a dinuclear asymmetric unit that is similar to that in complex **1** with the coordination of azide to the Ni^{II} ion instead of water. One Na^+ cation sits on the *facial* trisphenolate unit of the Ni_2L fragment, and N_3^- anion maintains the charge neutrality within the molecule. In all other respects, the asymmetric unit of **2** has a similar structural description as that of **1** and also exhibits similar metric parameters. The asymmetric units in **2** are interconnected through end-to-end[23] azide bridges between Ni2 and Na1, and the 1D chain[24] in complex $\{[Ni_2L(fp)(Na)(N_3)(H_2O)]\cdot5H_2O\}_n$ $(2\cdot5H_2O)_n$ is propagated (Figure 2).

Table 2. Selected interatomic distances [Å] and angles [°] for complex **3**.

Ni1–O4	2.009(5)	O2–Ni1–O5	169.2(2)
Ni1–N1	2.018(7)	O1–Ni1–O5	89.5(3)
Ni1–O2	2.026(5)	O4–Ni1–N2	96.0(2)
Ni1–O1	2.067(5)	N1–Ni1–N2	83.9(3)
Ni1–O5	2.069(7)	O2–Ni1–N2	91.9(2)
Ni1–N2	2.118(7)	O1–Ni1–N2	172.0(2)
Ni2–O3	2.006(5)	O5–Ni1–N2	92.0(3)
Ni2–N4	2.006(7)	O3–Ni2–N4	90.1(3)
Ni2–O4	2.057(5)	O3–Ni2–O4	91.9(2)
Ni2–O2	2.058(5)	N4–Ni2–O4	177.8(3)
Ni2–N3	2.189(7)	O3–Ni2–O2	91.2(2)
O6–Ni2	2.154(6)	N4–Ni2–O2	102.4(2)
Na1–O1	2.498(8)	O4–Ni2–O2	78.6(2)
Na1–O3	2.570(7)	O3–Ni2–O6	90.0(2)
		N4–Ni2–O6	87.0(3)
Ni1–O2–Ni2	96.3(2)	O4–Ni2–O6	92.0(2)
Ni1–O4–Ni2	96.9(2)	O2–Ni2–O6	170.6(2)
O4–Ni1–N1	175.3(3)	O3–Ni2–N3	173.0(2)
O4–Ni1–O2	80.5(2)	N4–Ni2–N3	83.1(3)
N1–Ni1–O2	104.2(3)	O4–Ni2–N3	94.9(2)
O4–Ni1–O1	91.9(2)	O2–Ni2–N3	88.7(2)
N1–Ni1–O1	88.4(2)	O6–Ni2–N3	91.2(3)
O2–Ni1–O1	88.0(2)	O7–Na1–O1	110.4(6)
O4–Ni1–O5	89.1(2)	O7–Na1–O3	109.4(6)
N1–Ni1–O5	86.2(3)	O1–Na1–O3	107.1(3)

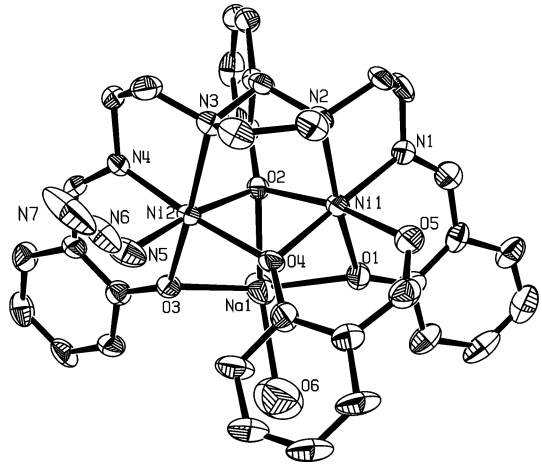

Figure 1. ORTEP representation of an asymmetric unit of $[Ni_2L(fp)(Na)(N_3)(H_2O)]$ (**2**) at the 50% probability level. Hydrogen atoms are omitted for clarity. Only independent non-carbon atoms are labeled.

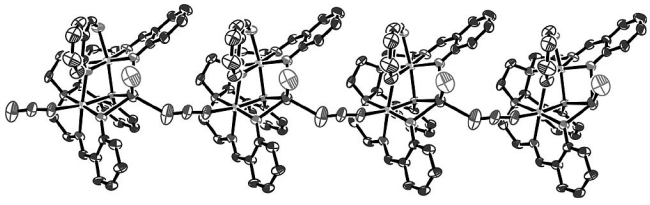

Figure 2. ORTEP representation of $\{[Ni_2L(fp)(Na)(N_3)(H_2O)]\cdot 5H_2O\}_n$ (**2**·$5H_2O$)$_n$ at the 50% probability level. Hydrogen atoms are omitted for clarity.

Complex **2** (Figure 1) is an aggregate of two Ni^{II} ions linked together by the N_4O_3 heptadentate ligand L^{3-} (Scheme 1). The bridging function is accomplished by the central imidazolidine group (NCN group) and phenoxide moiety (one μ-O atom) of L^{3-}, while the imine N atom and the phenoxide O donor at each side of the ligand occupy two additional coordination sites of each Ni^{II} center. An exogenous bidentate 2-formylphenolate (fp^-) ligand contributes to the bridging within the complex through the phenolate O donor and introduces asymmetry by binding to only one Ni atom through its carbonyl moiety. Hexacoordination around the other Ni ion is then achieved through the binding of an azide ion. The two Ni atoms are thus coordinated in distorted octahedral N_2O_4 and N_3O_3 environments; the two octahedra share the edge defined by the bridging phenolate oxygen atoms (Scheme S1). The planes intersecting at this edge form an angle of 153.37° as a result of the folding imposed by the imidazolidine ring [N2···N3 distance of 2.272(5) Å]. The geometric restrictions resulting from L^{3-} also lead to different Ni–O–Ni angles, 97.6(3)° and 99.2(3)° for the endogenous and exogenous phenolate oxygen atoms, respectively. The intramolecular Ni···Ni distance is 3.139(4) Å relative to 3.056 Å in complex **1**, which clearly indicates that this distance is increased as a result of 1D chain formation. The imidazolidine nitrogen atoms [Ni–N_{imd} (imd = imidazolidine) distances of 2.176(9) and 2.196(9) Å] are further away from Ni^{II} than the imine nitrogen atoms [Ni–N_{im} (im = imine) distances of 1.997(8) and 2.025(10) Å]. The O–Ni–O angles [78.7(3) and 77.1(3)°] within the metallacyclic $Ni_2(\mu\text{-}O)_2$ diamond core indicate distortions of the metal ion octahedra. The degree of distortion from an ideal octahedral (90°) geometry is reflected in the *cisoid* [105.2(3)–77.1(3)°] and the *transoid* [175.6(4)–166.5(3)°] angles. The bridging Ni–O(phenolate) distances (av. 2.073 Å) are longer than the terminal distances (av. 2.005 Å). The terminal Ni–O(carbonyl) and Ni–N(azide) distances are 2.099(8)° and 2.083(12) Å, respectively. The particular arrangement of L^{3-} around the Ni^{2+} ions leads to the formation of a [–O–Ni–O–Ni–O–] moiety (Figure 3 left) disposed so as to provide three facial donors that form an isosceles triangular face in order to favorably interact with the sodium ion through one oxygen atom of each of the phenolate groups [d(Na–O_{Ph}) = 2.264(9)–2.377(8) Å] (Scheme 3 left). These distances fall within the ranges observed for other metallacrowns or metallacryptates.[25] The sodium ion is found in an overall five-coordinate geometry (NO_4 donors); the three phenolate O atoms, a water O atom [d(Na–O6) = 2.513(16) Å], and a bridging azido N atom [d(Na–N7) = 2.364(19) Å]. Its coordination geometry can be viewed as a distorted square-pyramid in which the azido ligand is located in the apical position (Figure 3 right).

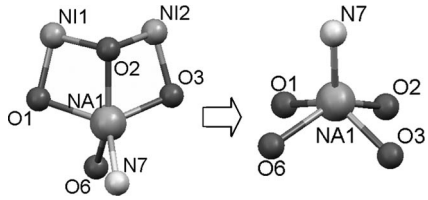

Figure 3. Left: the $NaNO_4Ni_2$ core in **2**; right: the square-pyramidal coordination environment around the Na^+ ion.

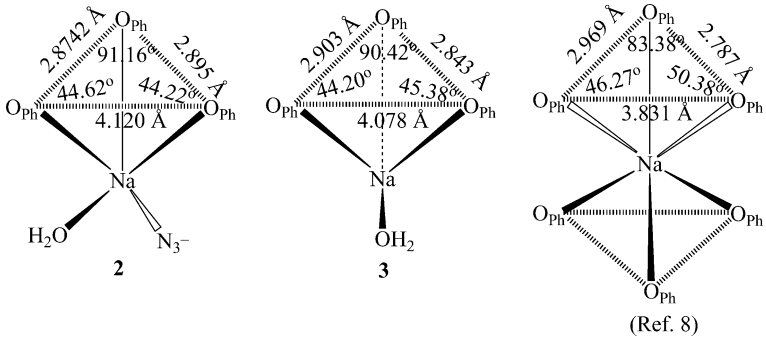

Scheme 3. Different coordination environments around Na^I. Left: the coordination of a trisphenolate isosceles triangular face within a $NaNO_4$ core in **2**; middle: the same O_3 triangular face within a NaO_4 core in **3**; right: the relative orientation of two such faces in a NaO_6 core in a reported Cu_4 complex (ref.[8]).

The staggered face-to-face orientation of two such triangular faces of the O donors of each ligand in $Cu_2L(N_3)$ is responsible for trapping the Na^+ cation in a distorted octahedral geometry, as reported earlier[8] (Scheme 3 right). Thus, the 1,3-bridging mode of the azido group between Ni and Na prevents any formation of a Ni_4-type cluster and leads to a 1D network with a Ni2···Na1 distance of 6.108 Å. The torsion angle around Ni2–N5–N7–Na1 is –89.09°, which indicates a *cis* bridging of N_3^- in a *gauche* conformation (Figure 4). The crystal-packing diagram along the crystallographic *a* axis is depicted in Figure S1.

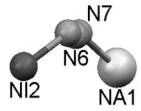

Figure 4. The *gauche* conformation of the N_3 bridge between Na and Ni.

The coordinated and lattice water molecules in **2** form an intermolecular hydrogen-bonded 2D network (Figure 5). Three of the five water molecules of crystallization [containing the O7, O8, O11 atoms] are involved in a zigzag intermolecular hydrogen-bonding network – the O6 atoms coordinated to the Na^+ ions connect two adjacent rows of azide-bridged 1D molecular chains made up of Ni2···Na1 units through a hydrogen-bonding network along the crystallographic *b* axis (Figure 6). The interatomic distances within this network are 2.78(3), 3.07(3), 2.70(3), and 2.82(3) Å, respectively, for the O6···O11, O11···O7, O7···O8, and O8···O6 interactions. The O7 atom is further hydrogen bonded with the template carbonyl oxygen atom O5 [O5···O7, 2.867(17) Å], which generates another network along the *a* axis (Figure 7). The remaining two water molecules of crystallization show strong hydrogen bonding [O9···O10, 2.43(4) Å], and O9 is further hydrogen bonded with the azide N7 nitrogen atom with a distance of 2.985(5) Å.

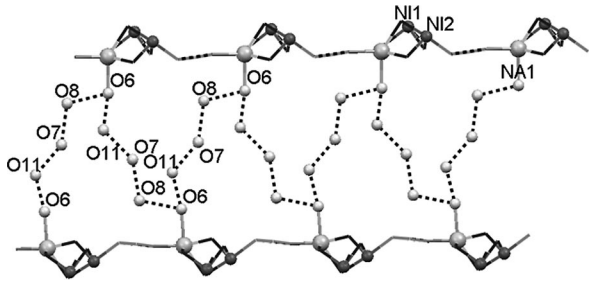

Figure 6. The hydrogen-bonded 1D water chain running along the crystallographic *b* axis between the two azido-bridged 1D molecular chains in **2**.

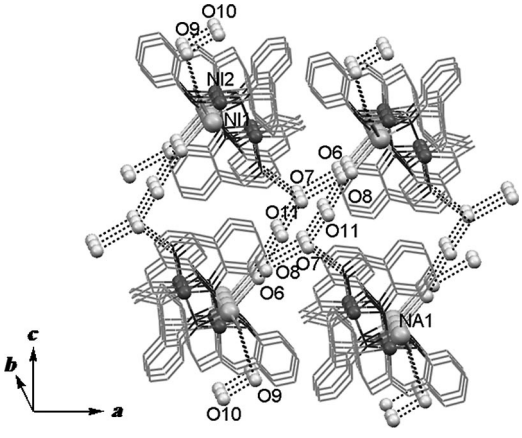

Figure 5. The intermolecular hydrogen-bonded 2D network viewed along an arbitary axis in **2**.

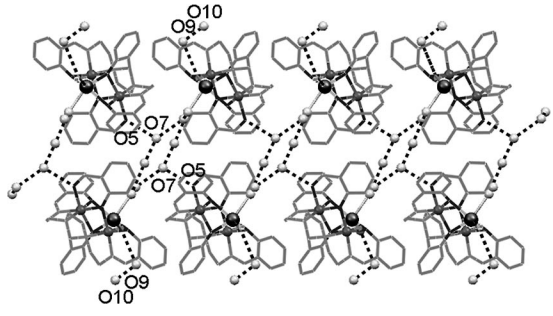

Figure 7. The hydrogen-bonded 1D chain connecting the $NaNi_2$ units along the crystallographic *a* axis in **2**. Ni: dark gray; O: light gray; Na: black.

[Ni_2(fp)LNa(H_2O)$_2$]·ClO_4·H_2O (3·ClO_4·H_2O)

The molecular structure of **3** reveals a $[Ni_2L(fp)Na(H_2O)_2]^+$ complex cation and a ClO_4^- anion with one water molecule of crystallization. Complex **3** (Figure 8) is a dinuclear aggregate of Ni^{II} ions bridged and chelated by the ligand L^{3-} in the same manner as in complex **2**, with the exception that one Na^+ cation is coordinated to two terminal phenolate oxygen atoms and one water molecule of crystallization.

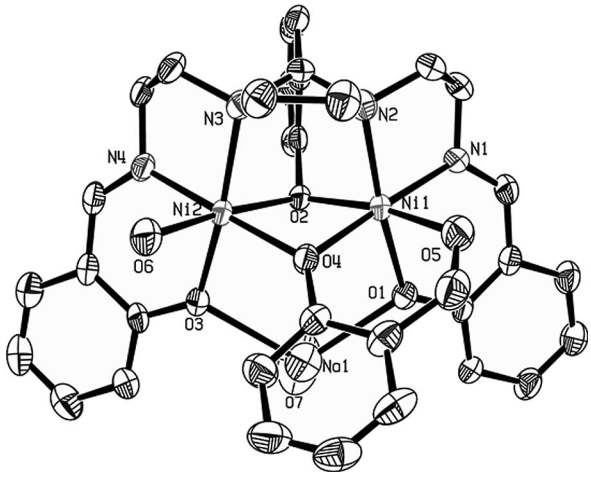

Figure 8. ORTEP representation of $[Ni_2L(fp)(Na)(H_2O)_2]^+$ (**3**) at the 40% probability level. Hydrogen atoms are omitted for clarity. Only independent non-carbon atoms are labeled.

An exogenous 2-formylphenolate (fp^-) ligand contributes to the bridging in the complex through the phenolate O donor and introduces asymmetry into the complex by binding to only one Ni atom through its carbonyl moiety. The Ni–O(carbonyl) distance of 2.069(7) Å is typical for this type of linkage, as in Ni–O(urea).[26] Hexacoordination around the other Ni ion is achieved through the binding of a molecule of water. Each Ni atom is thus coordinated in a distorted octahedral N_2O_4 environment; the two octahedra share the edge defined by the bridging phenolate oxygen atoms (Scheme S1). The planes intersecting at this edge form an angle of 152.46°, as a result of the folding imposed by imidazolidine ring [N2···N3 distance of 2.296(5) Å]. The O–Ni–O angles [80.5(2) and 78.6(2)°] within the metallacyclic $Ni_2(\mu\text{-}O)_2$ diamond core indicate distortions of the metal ion octahedra. The degree of distortion from an ideal octahedral (90°) geometry is reflected in the *cisoid* [104.2(3)–78.6(2)°] and the *transoid* [177.8(3)–169.2(2)°] angles. The Ni–O_{Ph} bond lengths are in the range 2.006(5)–2.154(6) Å. The bridging Ni–O(phenolate) distances (av. 2.037 Å) are comparable with the terminal distances (av. 2.036 Å). The terminal Ni–O(carbonyl) and Ni–O(water) distances are 2.069(7) Å and 2.154(6) Å, respectively. The geometric restrictions resulting from L^{3-} also lead to different Ni–O–Ni angles [96.3(2)° and 96.9(2)° for endogenous and exogenous phenolate oxygen atoms, respectively]. The intramolecular Ni···Ni distance is 3.042 Å and is comparable to 3.056 Å in complex **1**. The imidazolidine N atoms [Ni–N_{imd} distances of 2.118(7) and 2.189(7) Å] are further away from Ni^{II} than the imine N atoms [Ni–N_{im} distances of 2.006(7) and 2.018(7) Å]. The O_4 coordination environment around the Na^+ cation is a distorted tetrahedral with O–Na–O bond angles within the range 107.1(3)–110.4(6)°. The particular arrangement of L^{3-} around the metal ions provides three facial donors that form an isosceles triangular face such that they can favorably interact with the Na^+ ion (Scheme 3, middle), which is loosely held by the terminal phenolate O atoms of the Ni_2L fragment as evidenced from the Na–O_{Ph} bond lengths of 2.498(8) and 2.570(7) Å, which are comparable to the Na–O_{water} distance of 2.496(18) Å in **2**.

The central endogenous phenolate oxygen atom is 3.310 Å away from the Na^+ cation, which is longer than 2.388(9) Å in **2**. The oxygen atom (O6) of the coordinated water molecule to Ni^{II} is engaged in hydrogen bonding with the oxygen atom (O8) of the lattice water molecule and one of the oxygen atoms (O11) of the perchlorate anion with distances of 2.698 [O6···O8] and 3.028 Å [O6···O11], respectively (Figure 9). A crystal-packing diagram along the *b* axis is depicted in Figure S2.

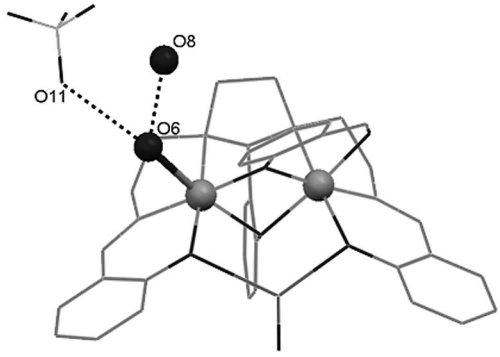

Figure 9. Intramolecular hydrogen bonding between the coordinated water molecule and the anion and the lattice water molecule viewed along an arbitary axis.

Magnetic Properties

{[Ni_2(fp)L(N_3)(Na)(H_2O)]·5H_2O}$_n$ (2·5H_2O)$_n$

The magnetic exchange within the 1D polymeric motif of complex **2** was investigated by means of bulk magnetization methods. Measurements were collected under a constant magnetic field of 0.5 T in the temperature range 4.5–300 K. The effective magnetic moment at 300 K of the 1D chain is 4.66 μ_B per molecule of the above complex; this value is 4.72 μ_B at 4.5 K. The plots of χ_M and μ_{eff} as a function of *T* for this complex are represented in Figure 10 (χ_M is the molar paramagnetic susceptibility and μ_{eff} is effective magnetic moment). At room temperature, χ_M is slightly higher than that expected for a pair of independent Ni^{II} ions with a *g* value of 2.29, and it increases upon cooling, with a more pronounced slope as the temperature approaches zero. This behavior clearly shows that the intramolecular coupling is ferromagnetic. The magnetic data were fitted by consider-

ing the intermolecular interactions. The model involves the use of a $\chi_M = f(T)$ expression [Equation (1)] derived from the Van Vleck equation.

$$\chi_M = \frac{2Ng^2\beta^2}{k(T-\theta)}\left[\frac{5+\exp(-4J/kT)}{5+3\exp(-4J/kT)+\exp(-6J/kT)}\right] \quad (1)$$

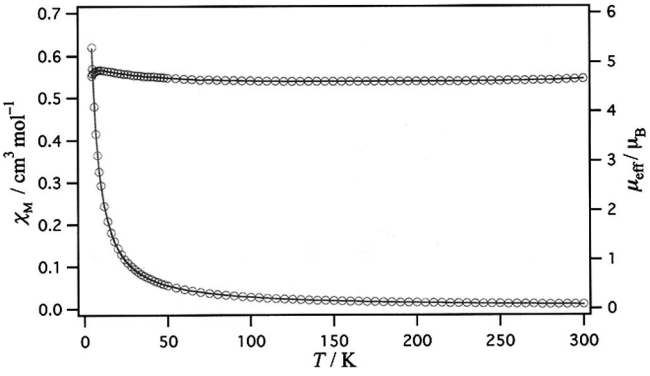

Figure 10. Plot of the temperature dependence of χ_M and μ_{eff} for **2**.

The parameters for this fit are $J = 2.02\ cm^{-1}$, $g = 2.29$, and $\theta = -1.7$ K. The small and ferromagnetic intramolecular coupling may be ascribed to the Ni–O–Ni angles formed by the phenolate bridges [between 97.6(3) and 99.0(3)°], which are within the range predicted for ferromagnetic interactions between the two nickel(II) ions, or to the imidazolidine –NCN– bridge, which also has been shown to facilitate ferromagnetic Ni···Ni exchange interaction.[17] The weak interdimer antiferromagnetic coupling is mediated by the Ni–$\mu_{1,3}$-N_3–Na···Ni bridges.

[Ni_2(fp)L(Na)(H_2O)$_2$]·ClO_4·H_2O (3·ClO_4·H_2O)

The magnetic exchange within the binuclear motif of complex **3** was investigated by means of bulk magnetization methods. Measurements were made under a constant magnetic field of 0.5 T in the temperature range 4.5–300 K. The effective magnetic moment at 300 K of the binuclear complex **3** is 4.54 μ_B per molecule of the above complex; this value is 4.99 μ_B at 4.5 K. The temperature dependence of the magnetic moment was analyzed by the same $\chi_M = f(T)$ expression [Equation (1)] as that for complex **2**. The plots of χ_M and μ_{eff} as a function of T for this complex are represented in Figure 11. The parameters for this fit are $J = 3.04\ cm^{-1}$, $g = 2.24$, and $\theta = -0.87$ K. This behavior clearly shows that the intramolecular coupling is ferromagnetic in nature.

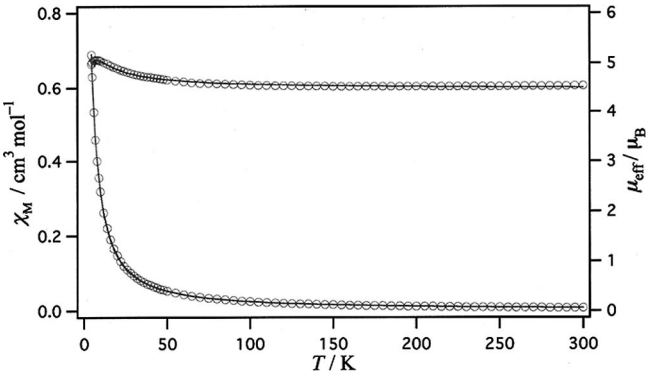

Figure 11. Plot of the temperature dependence of χ_M and μ_{eff} for **3**.

Concluding Remarks

As part of the interesting metal–ligand chemistry of L^{3-}, we have previously shown that reaction of H_3L with Ni^{II} on 2-formylphenolate as a template leads to the high yield formation of the terminal aqua coordinated neutral metalloligand [Ni_2(fp)L(H_2O)]·3H_2O (**1**·3H_2O) in the absence of any Na^+ source. Now we have shown that reaction of complex **1** with two different sodium salts produces counteranion–controlled, new, mixed-metal 1D chains {[Ni_2(fp)L(N_3)(Na)(H_2O)]·5H_2O}$_n$ (**2**·5H_2O)$_n$ and discrete $NaNi_2$ complexes [Ni_2(fp)L(Na)(H_2O)$_2$]·ClO_4·H_2O (**3**·ClO_4·H_2O) through the metallacrown-like coordination of Na^+ ions to the trisphenolate face of the Ni_2L fragments. Magnetic measurements indicate that complexes **2** and **3** exhibit ferromagnetic superexchange between the Ni^{II} centers to yield $S = 2$ ground states. We are currently working to exploit the asymmetry induced by the external template bridges in this reaction system to obtain heterometallic complexes.

Experimental Section

Materials and Physical Measurements: The chemicals used were obtained from the following sources: triethylenetetramine, sodium azide, and nickel nitrate hexahydrate from S.D. Fine Chem. (India) and 2-hydroxy benzaldehyde from SRL (India). All other chemicals and solvents were reagent grade materials and were used as received, without further purification. The elemental analyses (C, H, N) were performed with a Perkin–Elmer model 240C elemental analyzer. FTIR spectra were recorded with a Perkin–Elmer RX1 spectrophotometer. The solution electrical conductivity and electronic spectra were obtained by using a Unitech type U131C digital conductivity meter with a solute concentration of about 10^{-3} M and a Shimadzu UV 3100 UV/Vis/NIR spectrophotometer, respectively. The room temperature magnetic susceptibilities in the solid state were measured with a home-built Gouy balance fitted with a Polytronic d.c. power supply. The experimental magnetic susceptibilities were corrected for the diamagnetic response by using Pascal's constants. Magnetic measurements were carried out on polycrystalline samples (ca. 70 mg)with a Quantum Design MPMS-5S SQUID magnetometer operating at a constant magnetic field of 5000 G between 4.5–300 K. The experimental magnetic moment was corrected for the diamagnetic contribution from the sample holder and the diamagnetic response from the sample, which was evaluated from Pascal's constants.

General: All experimental procedures were carried out in air at room temperature. The ligand H_3L {2-(2′-hydroxyphenyl)-1,3-bis[4-(2-hydroxyphenyl)-3-azabut-3-enyl]-1,3-imidazolidine} was prepared according to a literature procedure.[19] Complex **1** was synthesized by a literature procedure.[17]

Table 3. Crystallographic data for complexes $(\mathbf{2}\cdot 5H_2O)_n$ and $\mathbf{3}\cdot ClO_4\cdot H_2O$.

Molecular formula	$C_{34}H_{44}N_7O_{11}NaNi_2$	$C_{34}H_{38}N_4O_{12}ClNaNi_2$
Molecular weight	867.13	870.51
Crystal system	monoclinic	monoclinic
Space group	$P2_1/a$	$P2_1/a$
a [Å]	19.069(2)	11.920(1)
b [Å]	9.036(1)	17.536(2)
c [Å]	22.108(3)	17.639(4)
β [°]	101.97(2)	91.79(2)
U [Å^3]	3726.6(8)	3685.4(10)
D_c [g cm^{-3}]	1.524	1.558
Z	4	4
F(000)	1760	1776
Crystal size [mm]	$0.32\times0.28\times0.26$	$0.28\times0.26\times0.22$
μ [mm^{-1}]	1.091	1.174
θ range [°]	1.88–24.97	1.15–24.97
R_1,[a] wR_2 [$I>2\sigma(I)$]	0.0933, 0.2506	0.0810, 0.2142
Goodness-of-fit on F^2	0.954	1.069
Final difference map max, min [e Å^{-3}]	0.875, –1.019	0.999, –1.147

[a] $R_1 = \Sigma(||F_o| - |F_c||)/\Sigma|F_o|$; $wR_2 = [\Sigma w(|F_o| - |F_c|)^2/\Sigma w(F_o)^2]^{1/2}$; $w = 0.75/[\sigma^2(F_o) + 0.0010F_o^2]$.

$\{[Ni_2L(fp)(N_3)(Na)(H_2O)]\cdot 5H_2O\}_n$ $(\mathbf{2}\cdot 5H_2O)_n$: A methanolic solution of NaN_3 (0.033 g, 0.52 mmol) was added dropwise to a CH_3CN solution (50 mL) of complex **1** (0.4 g, 0.52 mmol) over 15 min, and the mixture was stirred for 1 h. The resulting solution was filtered and left undisturbed so that the solvents could slowly evaporate. After 4 d, a green crystalline product was obtained (≈78% yield). The solid was isolated, washed with cold methanol, and dried under vacuum over P_4O_{10}. $C_{34}H_{44}N_7NaNi_2O_{11}$ (867.17): calcd. C 47.09, H 5.11, N 11.30; found C 46.89, H 5.24, N 11.18%. Molar conductance (MeCN solution): $\Lambda_M = 16\ \Omega^{-1}cm^2mol^{-1}$. UV/Vis spectrum ($CH_3CN$): λ_{max} (ε_{max}, $M^{-1}cm^{-1}$) = 932 (90), 783 (35), 603 (60), 375 (12605), 271 (17235) nm. Selected IR bands (KBr): $\tilde{\nu}$ = 3411 (br.), 2074 (s), 1639 (s), 1598 (s), 1535 (m), 1486 (m), 1447 (s), 1400 (m), 1341 (m), 1291 (m), 1150 (w), 760 (m) cm^{-1}.

$[Ni_2L(fp)(Na)(H_2O)_2]\cdot ClO_4\cdot H_2O$ $(\mathbf{3}\cdot ClO_4\cdot H_2O)$: A methanolic solution of $NaClO_4\cdot H_2O$ (0.073 g, 0.52 mmol) was added dropwise to a CH_3CN solution (50 mL) of **1** (0.4 g, 0.52 mmol) over 15 min, and the mixture was stirred for 1 h. The resulting solution was filtered and left undisturbed so that the solvents could slowly evaporate. After 7 d, a green crystalline product was obtained (≈75% yield). The solid was isolated, washed with cold methanol, and dried under vacuum over P_4O_{10}. $C_{34}H_{38}ClN_4NaNi_2O_{12}$ (870.51): calcd. C 46.91, H 4.39, N 6.43; found C 46.86, H 4.22, N 6.34. Molar conductance (MeCN solution): $\Lambda_M = 130\ \Omega^{-1}cm^2mol^{-1}$. UV/Vis spectrum ($CH_3CN$): λ_{max} (ε_{max}, $M^{-1}cm^{-1}$) = 922 (85), 783 (30), 510 (55), 375 (12870), 295(14485) nm. Selected IR bands (KBr): ν = 3421 (br.), 1642 (s), 1628 (s), 1600 (s), 1540 (m), 1484 (m), 1461 (m), 1445 (s), 1290 (m), 1121 (s), 758 (m) cm^{-1}.

X-ray Crystallographic Procedures for 2 and 3: Information concerning X-ray data collection and structure refinement of the compound is summarized in Table 3. The intensity data of the complexes **2** and **3** were collected on Nonius CAD4 X-ray diffractometer that uses graphite monochromated Mo-K_α radiation (λ = 0.71073 Å) by ω-scan method. Data were collected at 293 K. For complex **2**, total of 6680 reflections were recorded with Miller indices, h_{min} = 0, h_{max} = 22, k_{min} = 0, k_{max} = 10, l_{min} = –26, l_{max} = 25. For complex **3**, a total of 6724 reflections were recorded with Miller indices, h_{min} = 0, h_{max} = 14, k_{min} = 0, k_{max} = 20, l_{min} = –20, l_{max} = 20. In the final cycles of full-matrix least-squares on F^2 all non-hydrogen atoms were assigned anisotropic thermal parameters. The positions of the H atoms bonded to C atoms were calculated (C–H distance 0.97 Å). The structure was solved using the programme SHELX-97[27] and refined by full-matrix least-squares methods with use of the programme SHELX-97.[28] CCDC-628157 and -628158 for complexes **2** and **3** contain the supplementary crystallographic data for this paper. These data can be obtained free of charge from The Cambridge Crystallographic Data Centre via www.ccdc.cam.ac.uk/data_request/cif.

Supporting Information (see footnote on the first page of this article): The distorted octahedral N_2O_4 and N_3O_3 environments around the Ni centres in complexes **2** and **3** and the packing diagrams of complexes **2** and **3** are presented.

Acknowledgments

We are thankful to the Council of Scientific and Industrial Research, New Delhi, India for the financial support, and M. M. acknowledges the financial support by the "Open Research Center" Project for Private Universities: matching fund subsidy and Grants-in-Aid for Scientific Research No. 19550074 from the Ministry of Education, Culture, Sports, Science and Technology, Govt. of Japan.

[1] a) E. E. Moushi, T. C. Stamatatos, W. Wernsdorfer, V. Nastopoulos, G. Christou, A. J. Tasiopoulos, *Angew. Chem. Int. Ed.* **2006**, *45*, 7722–7725; b) E. E. Moushi, C. Lampropoulos, W. Wernsdorfer, V. Nastopoulos, G. Christou, A. J. Tasiopoulos, *Inorg. Chem.* **2007**, *46*, 3795–3797; c) M. Murugesu, W. Wernsdorfer, K. A. Abboud, E. K. Brechin, G. Christou, *Dalton Trans.* **2006**, 2285–2287; d) G. AromÌ, A. R. Bell, M. Helliwell, J. Raftery, S. J. Teat, G. A. Timco, O. Roubeau, R. E. P. Winpenny, *Chem. Eur. J.* **2003**, *9*, 3024–3032; e) D. M. J. Doble, C. H. Benison, A. J. Blake, D. Fenske, M. S. Jackson, R. D. Kay, W.-S. Li, M. Schröder, *Angew. Chem. Int. Ed.* **1999**, *38*, 1915–1918.

[2] C. Y. Huang, S. G. Rhee, P. B. Chock, *Annu. Rev. Biochem.* **1982**, *51*, 935–971.

[3] I. J. Hewitt, J.-K. Tang, N. T. Madhu, R. Clérac, G. Buth, C. E. Ansona, A. K. Powell, *Chem. Commun.* **2006**, 2650–2652.

[4] a) O. F. Schall, K. Robinson, J. L. Atwood, G. W. Gokel, *J. Am. Chem. Soc.* **1991**, *113*, 7434–7435; b) C. Chen, D. Huang, X. Zhang, F. Chen, H. Zhu, Q. Liu, C. Zhang, D. Liao, L. Li, L. Sun, *Inorg. Chem.* **2003**, *42*, 3540–3548; c) D. Cunningham, P. McArdle, M. Mitchell, N. N. Chonchubhair, M. O'Gara, *Inorg. Chem.* **2000**, *39*, 1639–1649.

[5] S. K. Dey, N. Mondal, M. S. E. Fallah, R. Vicente, A. Escuer, X. Solans, M. Font-Bardía, T. Matsushita, V. Gramlich, S. Mitra, *Inorg. Chem.* **2004**, *43*, 2427–2434.
[6] M. Bera, W. T. Wong, G. Aromí, D. Ray, *Eur. J. Inorg. Chem.* **2005**, 2526–2535.
[7] P. K. Nanda, G. Aromí, D. Ray, *Chem. Commun.* **2006**, 3181–3183.
[8] P. K. Nanda, G. Aromí, D. Ray, *Inorg. Chem.* **2006**, *45*, 3143–3145.
[9] M. Fondo, A. M. García-Deibe, M. Corbella, E. Ruiz, J. Tercero, J. Sanmartín, M. R. Bermejo, *Inorg. Chem.* **2005**, *44*, 5011–5020.
[10] M. Fondo, N. Ocampo, A. M. García-Deibe, M. Corbella, M. R. Bermejo, J. Sanmartín, *Dalton Trans.* **2005**, 3785–3794.
[11] M. Fondo, A. M. Garcia-Deibe, J. Sanmartin, M. R. Bermejo, L. Lezama, T. Rojo, *Eur. J. Inorg. Chem.* **2003**, 3703–3706.
[12] M. Bera, U. Mukhopadhyay, D. Ray, *Inorg. Chim. Acta* **2005**, *358*, 437–443.
[13] M. Bera, K. Biradha, D. Ray, *Inorg. Chim. Acta* **2004**, *357*, 3556–3562.
[14] P. K. Nanda, D. Mandal, D. Ray, *Polyhedron* **2006**, *25*, 702–710.
[15] P. K. Nanda, M. Bera, G. Aromí, D. Ray, *Polyhedron* **2006**, *25*, 2791–2799.
[16] M. Fondo, N. Ocampo, A. M. Garcia-Deibe, R. Vicente, M. Corbella, M. R. Bermejo, J. Sanmartin, *Inorg. Chem.* **2006**, *45*, 255–262.
[17] A. R. Paital, W. T. Wong, G. Aromí, D. Ray, *Inorg. Chem.* **2007**, *46*, 5727–5733.
[18] a) L. Balazs, H. J. Breunig, E. Lork, C. I. Rat, *Appl. Organomet. Chem.* **2005**, *19*, 1263–1267; b) G. L. Abbati, L.-C. Brunel, H. Casalta, A. Cornia, A. C. Fabretti, D. Gatteschi, A. K. Hassan, A. G. M. Jansen, A. L. Maniero, L. Pardi, C. Paulsen, U. Segre, *Chem. Eur. J.* **2001**, *7*, 1796–1807; c) R. W. Saalfrank, N. Low, B. Demleitner, D. Stalke, M. Teichert, *Chem. Eur. J.* **1998**, *4*, 1305–1311.
[19] E. Wong, S. Liu, T. Lugger, F. E. Hahn, C. Orvig, *Inorg. Chem.* **1995**, *34*, 93–101.
[20] M. Monfort, I. Resino, M. S. E. Fallah, J. Ribas, X. Solans, M. Font-Bardia, H. Stoeckli-Evans, *Chem. Eur. J.* **2001**, *7*, 280–287.
[21] a) M. Bera, W. T. Wong, G. Aromi, J. Ribas, D. Ray, *Inorg. Chem.* **2004**, *43*, 4787–4789; b) K. Nakamoto, *Infrared and Raman Spectra of Inorganic and Coordination Compounds*, 5th ed., Wiley & Sons, New York, **1997**.
[22] a) D. Nicholls in *Comprehensive Inorganic Chemistry* (Eds.: J. C. Bailar, H. J. Emeleus, R. Nyholm, A. F. Trotman-Dickenson), Pergamon, Oxford, **1973**, ch. 3, p. 1152; b) S. Mukhopadhyay, D. Ray, *Ind. J. Chem.* **1995**, *34A*, 466–468; c) T. Koga, H. Furutachi, T. Nakamura, N. Fukita, M. Ohba, K. Takahashi, H. Ōkawa, *Inorg. Chem.* **1998**, *37*, 989–996; d) M. Konrad, F. Meyer, A. Jacobi, P. Kircher, P. Rutsch, L. Zsolnai, *Inorg. Chem.* **1999**, *38*, 4559–4566.
[23] a) A. M. Madalan, M. Noltemeyer, M. Neculai, H. W. Roesky, M. Schmidtmann, A. Müller, Y. Journaux, M. Andruh, *Inorg. Chim. Acta* **2006**, *359*, 459–467; b) L. Fabrizzi, P. Pallavicini, L. Parodi, A. Perrotti, N. Sardone, A. Taglietti, *Inorg. Chim. Acta* **1996**, *244*, 7–9; c) A. Escuer, C. J. Harding, Y. Dussart, J. Nelson, V. McKee, R. Vicente, *J. Chem. Soc. Dalton Trans.* **1999**, 223–228.
[24] a) J. Ribas, A. Escuer, M. Monfort, R. Vicente, R. Cortés, L. Lezama, T. Rojo, *Coord. Chem. Rev.* **1999**, *193–195*, 1027–1068; b) M. Monfort, J. Ribas, X. Solans, M. Font-Bardia, *Inorg. Chem.* **1996**, *35*, 7633–7638; c) C. S. Hong, Y. Do, *Angew. Chem. Int. Ed.* **1999**, *38*, 193–195; d) R. Vicente, A. Escuer, J. Ribas, M. S. E. Fallah, X. Solans, M. Font-Bardia, *Inorg. Chem.* **1995**, *34*, 1278–1281.
[25] a) L. Y. Wang, S. Igarashi, Y. Yukawa, Y. Hoshino, O. Roubeau, G. Aromí, R. E. P. Winpenny, *Dalton Trans.* **2003**, 2318–2324; b) B. R. Gibney, H. Wang, J. W. Kampf, V. L. Pecoraro, *Inorg. Chem.* **1996**, *35*, 6184–6193.
[26] H. E. Wages, K. L. Taft, S. J. Lippard, *Inorg. Chem.* **1993**, *32*, 4985–4987.
[27] G. M. Sheldrick, *SHELXS-97, Program for the Solution of Crystal Structures*, University of Göttingen, Germany, **1997**.
[28] G. M. Sheldrick, *SHELXS-97, Program for the Refinement of Crystal Structures*, University of Göttingen, Germany, **1997**.

Received: July 3, 2007
Published Online: October 12, 2007

EurJIC European Journal of Inorganic Chemistry

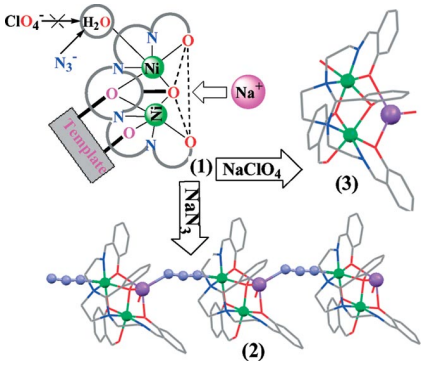

The reaction between the Ni_2 assembly on a formylphenolate template with a coordinated terminal water molecule and a capping imidazolidine ligand and N_3^- or ClO_4^- anions leads to two different types of products. The metallacrown-type coordination of the Na^+ cations results in new $NaNi_2$ complexes engaged in ferromagnetic interactions.

Keywords: Mixed-metal complexes / Imidazolidine / Dinuclear Ni^{II} complexes / Crystal structure / Magnetic properties

